

Superionic Adjustment Leading to Weakly Temperature-Dependent ZT Values in Bulk Thermoelectrics

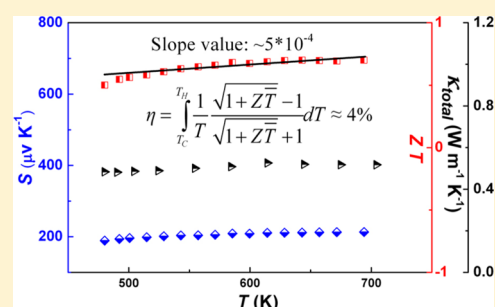
Hong Chen,[†] Hua Lin,[†] Zi-Xiong Lin,[†] Jin-Ni Shen,^{†,‡} Ling Chen,[†] and Li-Ming Wu^{*,†}

[†]State Key Laboratory of Structural Chemistry, Fujian Institute of Research on the Structure of Matter, Chinese Academy of Sciences, Fuzhou, Fujian 350002, People's Republic of China

[‡]University of Chinese Academy of Sciences, Beijing 100039, People's Republic of China

Supporting Information

ABSTRACT: Thermoelectric (TE) materials are of worldwide interest for energy sustainability through direct waste-heat-to-electricity conversion. Practically, a TE power generator requires a large working temperature gradient; to achieve high efficiency, key TE materials with high ZT values are necessary and, furthermore, their ZT values should decline as little as possible over the imposed temperature range. Unfortunately, sharp ZT declines in all of the known materials are inevitable. Here we found the bulk superionic α -Ag_{1-x}CuSe material exhibits unusual weakly temperature-dependent ZT values in the range of 480–693 K with the smallest ZT – T slope known to date. These result from the Seebeck coefficient balance of the countercontributions of holes and electrons and the weakly temperature-dependent thermal conductivity.



INTRODUCTION

The direct heat to electrical energy thermoelectric (TE) power generation technique faces a compelling need because of the worldwide energy crisis. Practically, a TE generator requires a large working temperature gradient (usually several hundred degrees); thus, to achieve high performance, key TE materials with high figure-of-merit (ZT) values are necessary and, furthermore, their ZT values should decline as little as possible within the working temperature gradient.^{1–5} Although high ZT peak values have been successfully realized in all of the well-known TE materials by several recent innovative strategies, sharp declines of ZT with temperature (as indicated by the slope of the ZT – T curve) are inevitable. According to the definition of the dimensionless $ZT = (S^2\sigma/\kappa)T$, where σ is the electrical conductivity, S is the Seebeck coefficient, κ is the thermal conductivity, and T is the absolute temperature, ZT is intrinsically temperature-dependent because the three parameters (S , σ , and κ) are all temperature-dependent. For example, sharp ZT value drops have been seen in PbTe from 2.2 at 900 K to 1.6 at 700 K,³ from 1.4 at 100 K to 0.8 at 250 K in Bi₂Te₃,⁴ and from 1.1 at 630 K to 0.4 at 430 K in Yb_{0.19}Co₄Sb₁₂.⁵ If the ZT – T slope can be reduced to half, the TE power generation efficiency will significantly increase 20–50%. This is indeed a big issue because the efficiency of a TE power generator (η) is given by $\eta = [(T_H - T_C)/T_H] \{ [(1 + ZT)^{1/2} - 1] / [(1 + ZT)^{1/2} + T_C/T_H] \}$, where T_H/T_C are the hot/cold-side temperatures and ZT is the arithmetic average of ZT_H and ZT_C .^{4,5} Unfortunately, the known TE materials cannot maintain their ZT peak values over the practically imposed work temperature difference. In order to avoid such a ZT decline with temperature and to improve the conversion efficiency, the

concept of functional gradient thermoelectric materials (FGTMs) was proposed earlier in the 1960s,⁶ which is to design composite FGTMs with different types of materials optimized for the TE properties over the specific temperature range. In 1993, Japan even initiated the second national project for research on such a subject. Although many theoretical works suggest that the conversion efficiency of FGTMs can increase about 50–100% in comparison with the single material,⁷ they face crucial problems in practice, such as severe diffusion of the segments leading to bad performance degradation and chemical, thermomechanical, and technological compatibility of the materials used in different segments. Besides, a complicated installation and assembling process, expensive cost, and low reliability are major difficulties for FGTMs over a broad temperature range.⁸

In this paper, we discover that superionic α -Ag_{1-x}CuSe exhibits unusual weakly temperature-dependent ZT values in the temperature range of 480–693 K with the smallest ZT – T slope of $\sim 5 \times 10^{-4}$ known to date. These are considered to result from the Seebeck coefficient balance of the countercontributions of holes and electrons and the weakly temperature-dependent thermal conductivity.

EXPERIMENTAL SECTION

All of the samples were prepared by solid-state reactions. The weighing manipulation was carried out in an argon-filled glovebox (moisture and oxygen levels of less than 0.1 ppm). An approximate total of 3 g of

Special Issue: To Honor the Memory of Prof. John D. Corbett

Received: September 4, 2014

Published: November 24, 2014

reactants (99.999% Ag, 99.999% Cu, and 99.5% Se, all purchased from Sinopharm Chemical Reagent Co., Ltd.) was mixed and loaded into an evacuated fused-silica tube under a residual pressure of $\sim 10^{-3}$ Pa. The assembly was heated to 1253 K over 54 h and subsequently cooled to room temperature. The products were well indexed as the orthorhombic $Pmmn$ phase (β - $\text{Ag}_{1-x}\text{CuSe}$, where $x = 0, 0.03$, and 0.06) without any detectable impurity according to the X-ray diffraction (XRD) patterns. When $x > 0.06$, impurity Cu_2Se was observed in the XRD patterns. The product ingot was ground and hot-pressed under 50 MPa at 823 K for 20 min in a graphite–steel mold with 15 mm internal diameter. The obtained pellets had relative densities of $\sim 95\%$ of the theoretical density. Such pellets were then cut into a cylinder disk with size of $\sim 2 \times 10$ mm and a rectangular bar with size of $\sim 2 \times 3 \times 8$ mm³ for thermal conductivity and transport property measurements, respectively. The confirmation powder XRD was taken after hot pressing on samples cut from the pellets. The XRD data were collected on a Miniflex II powder diffractometer with Cu $K\alpha$ radiation operating at 30 kV and 15 mA (2θ range from 25 to 65° with a step of 0.02°).

The thermal diffusivity (α) and specific heat capacity (C_p) were measured on a cylinder sample disk with size of $\sim 2 \times 10$ mm under an argon atmosphere at 300–693 K on a Netzsch LFA-457 MicroFlash instrument. The specific heat capacity, C_p , was derived using pyroceram as the standard according to $C_{p,\text{sam}} = C_{p,\text{std}}(\Delta U_{\text{std}}m_{\text{std}})/\Delta U_{\text{sam}}m_{\text{sam}}$, where ΔU_{std} and ΔU_{sam} are the detector signal differences of the standard and sample, respectively. The total thermal conductivity κ_{total} was calculated by $\kappa_{\text{total}} = \alpha C_p d$, where d is the measured density of the sample. The electrical conductivity (σ) and Seebeck coefficient (S) were measured simultaneously at 300–693 K under an argon atmosphere using the standard four-probe method with a ULVAC-RIKO ZEM-3 instrument system on a rectangular sample bar with size of $\sim 2 \times 3 \times 8$ mm³. Because AgCuSe melted at ~ 1053 K, when the measuring temperature was above 693 K, slight geometry deformation of the sample bar was observed; thus, a higher measuring temperature was not attempted. To confirm the reliability and repeatability of the data, the thermal and electrical property measurements were repeated 2–3 times. The data of each run showed consistency. After the measurement, the samples were ground and mounted for the confirmation XRD measurement. The XRD patterns before and after the TE measurement were consistent, indicating that no decomposition occurred.

RESULTS AND DISCUSSION

Silver copper selenide, AgCuSe , adopts an orthorhombic $Pmmn$ β -phase structure that transfers to a disordered α -phase structure around 473 K^{9,10} (Figure 1a, inset). α - AgCuSe has a rigid simple face-centered-cubic Se^{2-} sublattice and a highly disordered cation sublattice^{11,12} (Figure 1b).

Samples of $\text{Ag}_{1-x}\text{CuSe}$ ($x = 0, 0.03, 0.06$) were synthesized as an orthorhombic phase with a stoichiometric element mixture. The homogeneity has been confirmed by the XRD techniques,¹³ and no other impurity in the samples was detected (Figure 1a). The polycrystalline ingots were ground and then processed by hot pressing into dense pellets with a diameter of 15 mm ($>95\%$ of the theoretical density). These samples are stable in argon upon heating. The temperature-dependent electric-transport properties are shown in Figure 2a. A clear transition around 473 K is observed in both the $\rho(T)$ and $S(T)$ curves, which is in good agreement with the previous report indicating the orthorhombic-to-cubic phase transition.¹⁴ From 300 to 473 K, the resistivity increases from 0.5 to 2.5 m Ω cm, agreeing, in principle, with the previous report,¹⁴ and at the phase transition, a stepwise increase of ρ is observed, which may be related to the fact that the α phase has a wider energy gap.¹⁴ The resistivity of the α phase is 4.9–11.6 m Ω cm at 473–700 K in a nonmonotonic behavior, of which the descension before the turning point may be ascribed to the

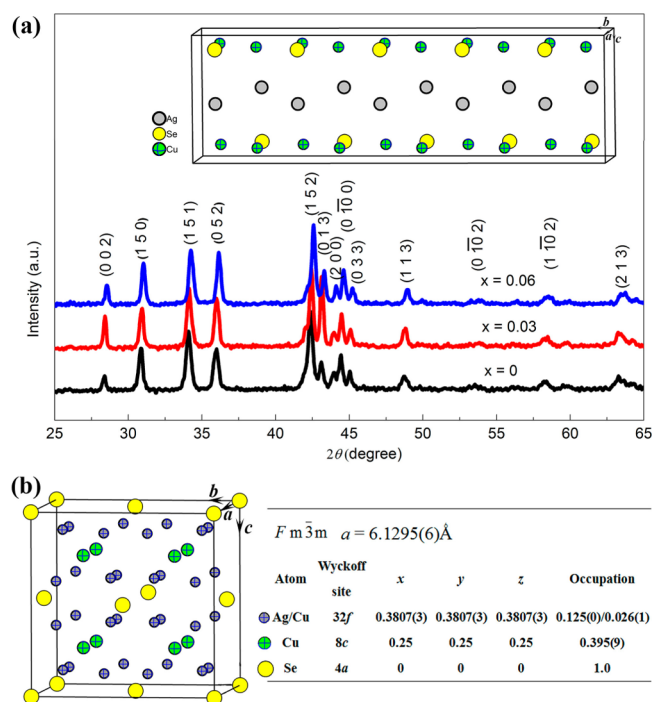


Figure 1. (a) Powder XRD patterns of the as-synthesized non-superionic β - $\text{Ag}_{1-x}\text{CuSe}$ at room temperature with diffraction peaks indexed. Inset: view of the unit cell with $a = 4.121$ Å, $b = 20.41$ Å, $c = 6.326$ Å, and space group $Pmmn$.¹³ (b) Unit cell of the superionic α - $\text{Ag}_{1-x}\text{CuSe}$, in which Ag^+/Cu^+ ions jointly disorder over the 32f sites (with occupancies of 0.125/0.026). Cu^+ ions also disorder over the 8c sites (with an occupancy of 0.395). The crystallographic data¹¹ are listed.

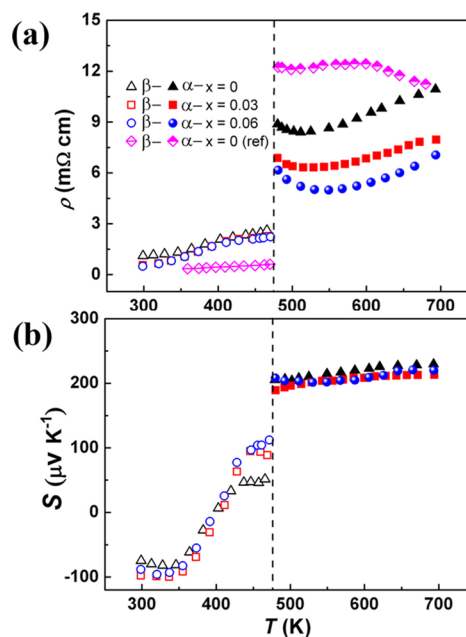


Figure 2. (a) Temperature-dependent resistivity (ρ) of $\text{Ag}_{1-x}\text{CuSe}$ ($x = 0, 0.03, 0.06$). The values reported in ref 14 are also presented for comparison. The same symbol notation for the samples is used in all panels. (b) Temperature-dependent Seebeck coefficient (S) of $\text{Ag}_{1-x}\text{CuSe}$ ($x = 0, 0.03, 0.06$). The vertical line (at 473 K) indicates the nonsuperionic-to-superionic phase transition.

fact that the defects are ionized gradually.¹⁴ After the defects are fully ionized, ρ increases with increasing temperature. As the silver vacancy concentration increases from $x = 0$ to 0.06, ρ systematically decreases. The resistivity of the α phase is comparable to those of the state-of-the-art TE materials.¹⁵ Because the resistivity is measured by the direct-current four-pole method, the ionic conductivity is blocked.

The Seebeck coefficient behavior of $\text{Ag}_{1-x}\text{CuSe}$ is much more complex than that of simple Ag_2Se or Cu_2Se . For Ag_2Se , before and after the superionic phase transition, S is negative.¹⁶ On the contrary, Cu_2Se exhibits positive S in both non-superionic and superionic regions.¹⁷ Differently, for $\text{Ag}_{1-x}\text{CuSe}$, S is negative in the nonsuperionic region (300–400 K) with a turning around 350 K, changes from negative to positive at 400 K, and reaches a plateau in the superionic region (480–693 K; Figure 2b). From 300 to 400 K, $\beta\text{-Ag}_{1-x}\text{CuSe}$ shows intrinsically electron-conducting behavior, as does Ag_2Se .¹⁷ The S curve of $\beta\text{-Ag}_{1-x}\text{CuSe}$ turns around 350 K, indicating that the electron-dominant behavior has been influenced by the holes. The S switches from negative to positive at 400 K, suggesting that the holes dominate over electrons at this point. From 350 to ~ 480 K, S increases almost linearly, as expected. At ~ 480 K, the material becomes superionic, $\alpha\text{-Ag}_{1-x}\text{CuSe}$, associated with an order-to-disorder structure change. In the superionic $\text{Ag}_{1-x}\text{CuSe}$ unit cell, the Ag–Se and Cu–Se bonding attractions can be easily overcome by the thermal energy, and both Ag and Cu ions are mobile. However, instead of linearly increasing with temperature, the S value of the superionic $\alpha\text{-Ag}_{1-x}\text{CuSe}$ exhibits an unusual weakly temperature-dependent feature. We suppose that this is caused by the fact that the increment rate of the hole concentration in such a region is not as fast as that before the superionic phase transition. Consequently, the positive S value is suppressed by the negative contribution from electrons cooperatively and ends up with a weakly temperature-dependent status. Similar S behavior was observed by Ishiwata et al.¹⁸ Although the intrinsic reason for this is still unclear, we believe that $\alpha\text{-Ag}_{1-x}\text{CuSe}$ is an ideal system, where the superionic concentration plays an important role in adjusting the TE property.

The calculated power factors (PFs) are shown in Figure 3. In the $\beta\text{-Ag}_{1-x}\text{CuSe}$ region, the PF decreases rapidly from 17 to $5 \mu\text{W cm}^{-1} \text{K}^{-2}$ owing to the increasing resistivity and decreasing absolute value of S . In the 400–473 K range, the PF increases with the temperature. After the phase transition, the PF of the $\alpha\text{-AgCuSe}$ phase is slightly temperature-dependent owing to the slowly increased ρ and weakly temperature-dependent S .

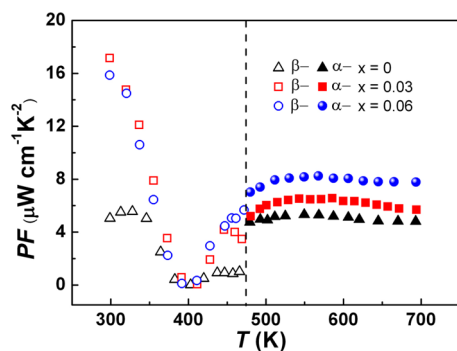


Figure 3. Temperature-dependent PF of $\text{Ag}_{1-x}\text{CuSe}$ ($x = 0, 0.03, 0.06$). The vertical line (at 473 K) indicates the nonsuperionic-to-superionic phase transition.

Besides, the PF of $\alpha\text{-Ag}_{1-x}\text{CuSe}$ slightly increases from 7.4 to $8.2 \mu\text{W cm}^{-1} \text{K}^{-2}$ as the silver vacancy concentration varies from $x = 0$ to 0.06.

The temperature dependence of the total thermal conductivity (κ_{total}) is shown in Figure 4a (the thermal diffusivity α and special heat capacity C_p are listed in Figures S1 and S2 in the Supporting Information, SI). At room temperature, κ_{total} is $1.4\text{--}1.9 \text{ W m}^{-1} \text{K}^{-1}$. After the phase transition, κ_{total} decreases to $0.5\text{--}0.6 \text{ W m}^{-1} \text{K}^{-1}$. The lattice thermal conductivity (Figure 4c) was evaluated by subtracting the electronic contribution ($\kappa_{\text{ele}} = L\sigma T$, where the Lorenz number $L = 1.5 \times 10^{-8} \Omega \text{ W K}^{-2}$ for nondegenerate materials¹⁹ and the carrier concentrations were measured to be $(4.1\text{--}7.5) \times 10^{18} \text{ cm}^{-3}$ for $x = 0.04, 0.045, 0.05$, the as-synthesized samples; Figure 4b). κ_{latt} is almost temperature-independent at the α phase. For example, for $\alpha\text{-Ag}_{1-x}\text{CuSe}$ (above 480 K), where $x = 0$, it maintains a value of $0.41 \pm 0.02 \text{ W m}^{-1} \text{K}^{-1}$ (Figure 4c). Similar to those in AgSbTe_2 and AgBiSe_2 ,²⁰ such behavior should correlate with atom disordering in the lattice, leading to extremely high anharmonicity, which limits the phonon thermal conductivity to its minimum possible value, where the free path equals the interatomic distance. The inelastic neutron scattering spectral studies of the AgCuSe system show that this system has a high level of anharmonicity.^{10,11} As a result, scattering could intrinsically limit the lattice thermal conductivity. Of course, the ion contribution is not ignorable.²¹

The weakly temperature-dependent ZT of the superionic $\alpha\text{-AgCuSe}$ is due to the weakly temperature-dependent S and κ_{total} and very gentle change of ρ with the temperature (Figure 4d). $\alpha\text{-Ag}_{1-x}\text{CuSe}$ ($x = 0$) realizes a linear fitted $ZT\text{--}T$ slope of $\sim 5 \times 10^{-4}$ (the fitting equations are listed in Figure S3 in the SI), which is 4–12 times lower than those of the well-known TE materials. For instance, PbTe shows the record high ZT of 2.2 at 915 K, which declines with a slope of 38×10^{-4} to 470 K.³ If a known TE material adopts a flat $ZT\text{--}T$ slope as $\alpha\text{-AgCuSe}$ does, to achieve its current efficiency, ZT_{max} only requires 1.13 instead of 2.2 for PbTe ³ or 1.11 instead of 1.5 for TAGS.²²

As the silver vacancy concentration varies from $x = 0$ to 0.06, the ZT value increases from 0.6 to 0.9, and the corresponding $ZT\text{--}T$ slope increases from about 5 to 12×10^{-4} (Figure 4d; the solid line is the linear fitting). These suggest that varying the silver content may optimize the balance among the key parameters and enhance the ZT values while keeping their temperature-independent feature.

The temperature-independent ZT values are of great significance. Merely a high ZT peak value does not always mean high efficiency; what really matters is the average ZT value over the imposed working temperature gradient. If $T_{\text{H}} = 693$ K and $T_{\text{C}} = 480$ K are assumed, for AgBiSe_2 with a ZT_{max} of ~ 1.5 at 693 K but 0.02 at 480 K,²³ an efficiency of only 2.3% is obtained (Table 1). Owing to the small $ZT\text{--}T$ slope change, $\alpha\text{-AgCuSe}$ with a relatively small $ZT_{\text{max}} = 0.6$ at 693 K can achieve significant efficiency with a 74% increase in comparison with that of AgBiSe_2 .²³

CONCLUSION

In conclusion, the unusual weakly temperature-dependent ZT value in bulk superionic $\alpha\text{-Ag}_{1-x}\text{CuSe}$ ($x = 0, 0.03, 0.06$) demonstrates itself as a promising system to study the TE properties. Such $ZT\text{--}T$ behavior of $\alpha\text{-Ag}_{1-x}\text{CuSe}$ is due to the weak temperature dependence of the Seebeck coefficient (S) and thermal conductivity (κ_{total}) and the very gentle change of the electrical conductivity (ρ) with the temperature. The S

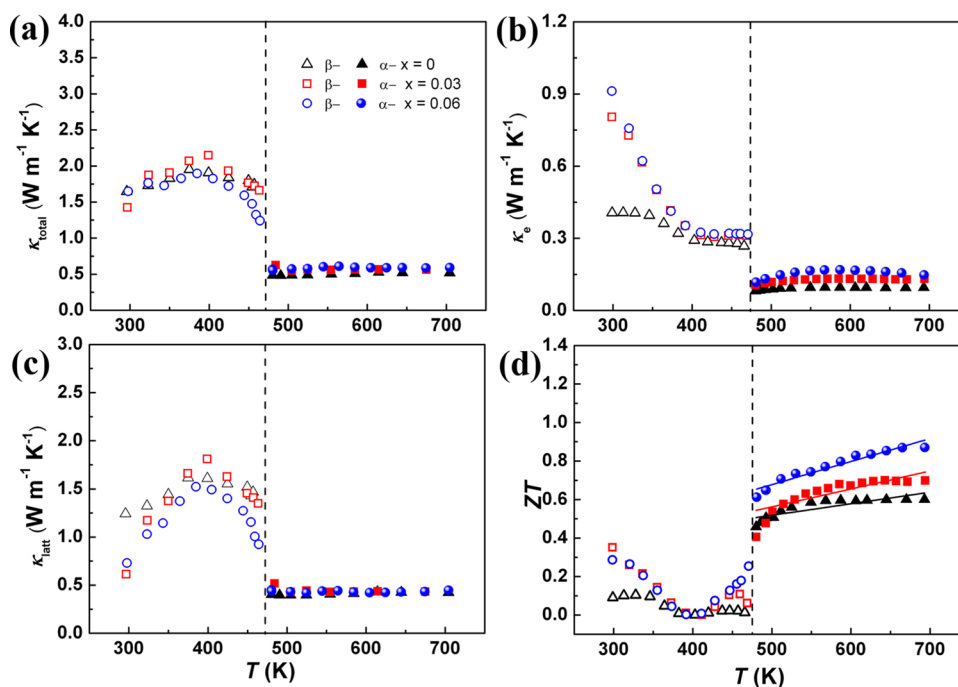


Figure 4. Temperature-dependent thermal conductivity and ZT value of $\text{Ag}_{1-x}\text{CuSe}$ ($x = 0, 0.03, 0.06$). Total thermal conductivity (κ_{total} , a), electronic thermal conductivity (κ_e , b), and lattice thermal conductivity (κ_{latt} , c). (d) Figure of merit (ZT). The solid line is the linear fitting of the ZT - T slope of the superionic $\alpha\text{-Ag}_{1-x}\text{CuSe}$. The fitting equations are listed in Figure S3 in the SI. The vertical line (at 473 K) indicates the nonsuperionic-to-superionic phase transition.

Table 1. Performance Parameters of Selected TE Materials

compound		ZT_{max}	ZT at 480 K	ZT at 693 K	slope ^a ($\times 10^{-4}$)	η (%) ^b
AgBiSe_2 ²³		1.5 at 700 K	~0.02	~1.5	~63	~2.3
$\alpha\text{-Ag}_{1-x}\text{CuSe}$ (this work)	$x = 0$	0.6 at 693 K	~0.5	~0.6	~5	~4.0
	$x = 0.03$	0.7 at 693 K	~0.4	~0.7	~9	~4.4
	$x = 0.06$	0.9 at 693 K	~0.6	~0.9	~12	~5.0

^aSlope of the ZT - T curve representing degradation of the ZT value as a function of the temperature. The linear fitting range is from 480 to 693 K. ^b $\eta = \int_{T_C}^{T_H} (1/T) \{ [(1 + ZT)^{1/2} - 1] / [(1 + ZT)^{1/2} + 1] \} dT$; $T_H = 693$ K and $T_C = 480$ K.

value may be balanced by two types of carriers (holes and electrons), and the κ_{total} value is due to the extremely high anharmonicity of the structure. When the phase becomes superionic, the increment rate of the hole concentration is not as fast as that before the phase transition. Consequently, the positive S value is suppressed by the negative contribution from the electrons. The intrinsic reason for this is worthy of further study. The superionic concentration may play an important role in optimizing the TE temperature-dependent properties. With the advance of the weakly temperature-dependent ZT value, we can expect a substantial performance enhancement in the TE power generator in a considerably wide working temperature gradient and an enhancement of the conversion efficiency of 74% or higher.

■ ASSOCIATED CONTENT

Supporting Information

Thermal diffusivity, specific heat capacity, and ZT - T slope fitting. This material is available free of charge via the Internet at <http://pubs.acs.org>.

■ AUTHOR INFORMATION

Corresponding Author

*E-mail: liming_wu@fjirsm.ac.cn. Tel: (011)86-591-63173211.

Notes

The authors declare no competing financial interest.

■ ACKNOWLEDGMENTS

This research was supported by the National Natural Science Foundation of China under Projects 20973175, 21225104, 21233009, and 21301175 and the “Knowledge Innovation Program of the Chinese Academy of Sciences” (Grant KJCX2-YW-H20). We thank the anonymous reviewers for their constructive comments. We thank Prof. Mercouri G. Kanatzidis at Northwestern University, Evanston, IL, for helpful discussions.

■ REFERENCES

- (1) Goldsmid, H. J. In *CRC Handbook of Thermoelectrics*; Rowe, D. M., Eds.; CRC Press: Boca Raton, FL, 1995; Chapter 3.
- (2) DiSalvo, F. J. *Science* **1999**, *285*, 703–706.
- (3) Biswas, K.; He, J. Q.; Blum, I. D.; Wu, C. I.; Hogan, T. P.; Seidman, D. N.; Dravid, V. P.; Kanatzidis, M. G. *Nature* **2012**, *489*, 414–418.
- (4) Poudel, B.; Hao, Q.; Ma, Y.; Lan, Y.; Minnich, A.; Yu, B.; Yan, X.; Wang, D.; Muto, A.; Vashaee, D.; Chen, X.; Liu, J.; Dresselhaus, M. S.; Chen, G.; Ren, Z. *Science* **2008**, *320*, 634–638.
- (5) Nolas, G. S.; Kaeser, M.; Littleton, R. T.; Tritt, T. M. *Appl. Phys. Lett.* **2000**, *77*, 1855–1857.

- (6) Ioffe, A. F. Thermoelectric battery. USSR Patent 126158, Jan 1, 1960.
- (7) Hirano, T.; Whitlow, L. W.; Miyajima, M. In *Ceramic Transactions*; Holt, J. B., Koizumi, M., Hirai, T., Munir, Z. A., Eds.; American Ceramic Society: Westerville, OH, 1993; Vol. 34, pp 23–30.
- (8) Vikhor, L. M. J. *Thermoelectr.* **2005**, *1*, 7–21.
- (9) Tomotaka, S.; Masaji, A.; Takashi, S. *Proceedings of the 1st International Discussion Meeting on Superionic Conductor Physics*, Kyoto, Japan, Sept 10–14, 2003; World Scientific Publishing: Singapore, 2007.
- (10) Trots, D. M.; Skomorokhov, A. N.; Knapp, M.; Fuess, H. *Eur. Phys. J. B* **2006**, *51*, 507–512.
- (11) Bikkulova, N. N.; Beskrovnyoe, A. I.; Yadrovskioe, E. L.; Skomorokhov, A. N.; Stepanov, Y. M.; Mikolaoechuk, A. N.; Sagdatkireeva, M. B.; Karimov, L. Z. *Crystallogr. Rep.* **2007**, *52*, 453–455.
- (12) Boyce, J. B.; Huberman, B. A. *Phys. Rep.* **1979**, *51*, 189–265.
- (13) Ohtani, T.; Maruyama, K.; Ohshima, K. *Mater. Res. Bull.* **1997**, *32*, 343–350.
- (14) Miyatani, S. Y.; Miura, Y. C.; Ando, H. *J. Phys. Soc. Jpn.* **1979**, *46*, 1825–1832.
- (15) Sootsman, J. R.; Chung, D. Y.; Kanatzidis, M. G. *Angew. Chem., Int. Ed.* **2009**, *48*, 8616–8639.
- (16) Day, T.; Drymiotis, F.; Zhang, T.; Rhodes, D.; Shi, X.; Chen, L.; Snyder, G. J. *J. Mater. Chem. C* **2013**, *1*, 7568–7573.
- (17) Liu, H.; Shi, X.; Xu, F.; Zhang, L. L.; Zhang, W. Q.; Chen, L. D.; Li, Q.; Uher, C.; Day, T.; Snyder, G. J. *Nat. Mater.* **2012**, *11*, 422–425.
- (18) Ishiwata, S.; Shiomi, Y.; Lee, J. S.; Bahramy, M. S.; Suzuki, T.; Uchida, M.; Arita, R.; Taguchi, Y.; Tokura, Y. *Nat. Mater.* **2013**, *12*, 512–517.
- (19) Goldsmid, H. J. *Applications of thermoelectricity*; Butler & Tanner Ltd.: London, 1960.
- (20) Morelli, D. T.; Jovovic, V.; Heremans, J. P. *Phys. Rev. Lett.* **2008**, *101*, 035901.
- (21) Yonashiro, K.; Tomoyose, T.; Sakai, E.; Yamashiro, M.; Kobayashi, M. *Solid State Ionics* **1988**, *28*, 152–55.
- (22) Yang, S. H.; Zhu, T. J.; Sun, T.; He, J.; Zhang, S. N.; Zhao, X. B. *Nanotechnology* **2008**, *19*, 245707.
- (23) Xiao, C.; Qin, X. M.; Zhang, J.; An, R.; Xu, J.; Li, K.; Cao, B. X.; Yang, J. L.; Ye, B. J.; Xie, Y. *J. Am. Chem. Soc.* **2012**, *134*, 18460–18466.